

**Subject Areas:**

xx, xxx, xxx

Keywords:

nonlinear elasticity, planets, instability

Author for correspondence:

A. Goriely

e-mail: goriely@maths.ox.ac.uk

On the Figure of Elastic Planets I: Gravitational Collapse and Infinitely Many Equilibria

Fei Jia^{1,2}, Ousmane Kodio², S. Jon Chapman², Alain Goriely²

¹School of Manufacturing Science and Engineering, Southwest University of Science and Technology, Sichuan 621010, China; ²Mathematical Institute, University of Oxford, Oxford OX2 6GG, UK.

A classic problem of elasticity is to determine the possible equilibria of an elastic planet modelled as a homogeneous compressible spherical elastic body subject to its own gravitational field. In the absence of gravity the initial radius is given and the density is constant. With gravity and for small planets, the elastic deformations are small enough so that the spherical equilibria can be readily obtained by using the theory of linear elasticity. For larger or denser planets, large deformations occur and the general theory of nonlinear elasticity is required to obtain the solution. Depending on the elastic model, we show that there may be parameter regimes where there exist no equilibrium or arbitrarily many equilibria. Yet, at most two of them are dynamically stable with respect to radial disturbances. In some of these models, there is a critical initial radius at which spherical solutions cease to exist. For planets with larger initial radii, there is no spherical solution as the elastic forces are not sufficient to balance the gravitational force. Therefore, the system undergoes gravitational collapse, an unexpected phenomenon within the framework of classical continuum mechanics.

1. Introduction

Understanding the deformations of solid planets in a gravitational field is a central problem of celestial mechanics and planetary sciences. It is essential for the theory of seismic waves [1–3] and is related to the phenomenon of “earth tides” [4,5], the displacement of the earth’s solid surface by gravity which is used as a

© The Authors. Published by the Royal Society under the terms of the Creative Commons Attribution License <http://creativecommons.org/licenses/by/4.0/>, which permits unrestricted use, provided the original author and source are credited.

method to probe the composition of planets and moons [6–9]. Most of the studies in these fields relate to aspherical deformations due to the gravitational interactions of many bodies or are related to the problem of accretion and formation of heavenly bodies [10]. Yet, the first and simplest problem of determining the spherical equilibria of an isotropic homogeneous elastic body under its own gravitational field seems to have been overlooked. Despite its apparent simplicity, we will show that it hides many surprises.

To define the problem, we consider a Newtonian universe with a single continuum body. In the absence of gravity, this body, in the reference configuration, has constant density and is a stress-free, isotropic, compressible hyperelastic sphere of radius R_0 . Now, consider the same body subject to a body force created by its own gravitational field. We will simply refer to this body as an *elastic planet*. The problem is then to find all possible spherical equilibria in the current configuration. Simply put: what is the radius of an elastic planet? While it is clear that an actual planet in the known universe is a much more complicated object, understanding this ideal problem is of fundamental interest before further effects can be considered.

The problem of identifying the shape (or “figure”) of a continuum body under its own gravity field is as old as the theory of gravity itself as Newton already worked on the problem in the fluid case in 1687 (*Principia*, Book 1, Section XIII, see Fig. 1). Newton applied his theory to estimate the flattening of the Earth due to its rotation. In particular, the question of whether the Earth is oblate or prolate was a topic of the greatest interest in learned circles with Newton and Maupertuis on the oblate side of the argument and Descartes and the Cassinis on the prolate one. The question was eventually settled with Maupertuis’ famous expedition to Lapland in 1736 [11] from which he earned the name “le grand aplatisseur” (“the great flattener”). In the 18th and early 19th Century, this problem received considerable attention with contributions from Clairaut, Stirling, John and Daniel Bernoulli, MacLaurin, Euler, d’Alembert, Buffon, Jacobi, Lagrange, Cavendish, Laplace, Young, Biot, Gauss, Poisson, Cauchy, Airy, Sturm. In *A History of the Mathematical Theories of Attraction and the Figure of the Earth*, Todhunter summarises the various contributions to the field up to 1873 in two volumes and 929 pages [12]. Yet, by 1873 the story was far from over and the general problem of determining the shape and stability of a fluid body under gravitation and rotation remained a central scientific issue in the late 19th Century and early 20th Century through the work of Meyer, Liouville, Dirichlet, Roche, Dedekind, Kelvin, Tait, Jeans, Appell, Riemann, Poincaré, and Cartan [13,14]. This line of research culminated with the seminal work of Chandrasekhar [15] summarised in his book *Ellipsoidal Figures of Equilibrium* [16] and remains of current interest [17,18].

By comparison, the equivalent problem for a solid or elastic planet has received considerably less attention. It was first studied by William Thomson (Lord Kelvin) in 1863 in his argument for the existence of Earth’s tides and for a short while became a hot topic of research with key contributions by George Darwin [4], James Jeans [20–22], and Augustus Love [23] with his Adams’ prize winning essay *Some Problems of Geodynamics* published in 1911 in which “Love’s numbers” characterising the height of a tidal deformation are discussed (see historical review in [24] and Fig. 1).

Despite these important contributions, the study of elastic planets and their stability encountered fundamental difficulties due to the lack of a general theory of elasticity at the time and, in particular, the problem of handling initial stress. To circumvent these problems a number of simplifying assumptions were made. The researchers at the time were honest in the ultimate justification of these assumptions made in order to make progress in the mathematical analysis. As Love writes: “The problem thus posed is an artificial one, which may, nevertheless, throw light on the actual problem” [23]. We briefly comments on three classic assumptions:

The assumption of isostasy. This assumption simply states that the body is in a state of hydrostatic stress. Love [25] justifies this assumption by assuming that a solid planet is made of a viscous fluid with a crust, and by further assuming that the differences between stress components in the crust are relatively small. This is a crucial assumption that completely changes the nature of the problem into a problem much more closely related to a fluid planet than an elastic planet.

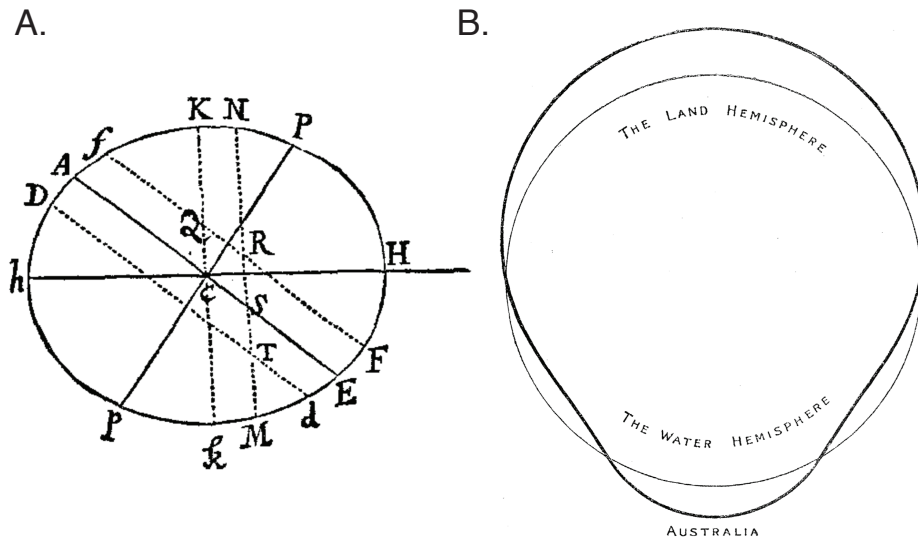


Figure 1. A. Newton's computation of oceanic fluid tides [19] and B. Jeans' computation of Earth's solid tides [20].

The assumption of constant density: We define two densities, the *natural density*, the density of the material in a stress-free state (without gravity), and the *current density*, the density of the material in the current configuration (with gravity). The classic assumption is related to the current density as the equations for the stresses are simpler. In the typical case of constant current density, it implies that the material at the centre of the planet has a lower natural density than the material at the rim. An assumption on the current density is therefore an assumption on the *structure* and not the *material*. It assumes that we have some knowledge of the state of deformation of the final material rather than on the material that makes up the body. While it may be appropriate as an approximation, it does not seem particularly fruitful as a theoretical construct and precludes the comparison of planets of different radii as they would be made of different materials.

The assumption of small strains: If the strains are small enough, the problem is greatly simplified and the theory of linear elasticity can be used. If, in addition, the density is assumed to remain constant in all deformations, the problem can be formulated in the current coordinates and can be easily solved as shown by Love [26] (and given as an exercise in Landau & Lifshitz [27]).

Around 1917, following the work of Jeans [22] who concluded that elastic planets are always stable, the problem of elastic planets went into a coma. It was only resurrected with the development of nonlinear elasticity following WWII when the exact problem of determining the shape of a body under its own gravitational field, as given in the next Section, was first formulated by Sawyers and Rivlin in the context of seismic waves [2].

2. Model

(a) The general problem

Before looking at the specific problem of radial equilibria, we present the general problem following the notation in [28]. We consider an initial, stress-free, body $\mathcal{B}_0 \subset \mathbb{R}^3$ with a given *natural density* $\rho_0 = \rho_0(\mathbf{X})$ where $\mathbf{X} \in \mathcal{B}_0$ denotes the reference position of a material point. This configuration defines the shape of the body in the absence of loads and body forces. It is therefore suitable as a reference configuration and can be used to compute elastic equilibria. In the presence of loads and/or body forces, the body deforms into a new configuration $\mathcal{B} \subset \mathbb{R}^3$ and

we assume the existence of an invertible map $\chi : \mathcal{B}_0 \rightarrow \mathcal{B}$ so that $\mathbf{x} = \chi(\mathbf{X})$, where \mathbf{x} denotes the current position of a material point, initially at the position \mathbf{X} . Assuming that the deformation is sufficiently smooth, we define the *deformation gradient*

$$\mathbf{F} = \text{Grad}(\chi), \quad (2.1)$$

where $\text{Grad}(\cdot)$ denotes the gradient in the reference coordinates. The determinant $J = \det \mathbf{F} > 0$ represents the local change of volume. The equations of equilibrium are given by the Cauchy equations for the Cauchy stress tensor

$$\text{div} \mathbf{T} + \rho \mathbf{b} = \mathbf{0}, \quad (2.2)$$

where the divergence $\text{div}(\cdot)$ is taken in the current coordinates, $\rho = \rho_0/J$ is the current density and \mathbf{b} is the body force. In the case of gravitational interaction, this body force is given through the gravitational potential, U by [29]

$$\mathbf{b} = \text{grad } U, \quad \text{with} \quad U = -G \int_{\mathcal{B}} \frac{\rho(\mathbf{y})}{|\mathbf{x} - \mathbf{y}|} d\mathbf{y}, \quad \mathbf{x} \in \mathcal{B}, \quad (2.3)$$

where $G \approx 6.67410^{-11} \text{m}^3 \text{kg}^{-1} \text{s}^{-2}$ is the universal gravitational constant. To close the system we have to relate the Cauchy stress tensor to the deformation gradient. Here, we assume that the material is hyperelastic. This implies that there exists a strain-energy density function $W = W(\mathbf{F})$ such that

$$\mathbf{T} = \frac{1}{J} \mathbf{F} \frac{\partial W}{\partial \mathbf{F}}. \quad (2.4)$$

The strain-energy density function satisfies the ellipticity conditions in small strains and is assumed to be objective so that the system satisfies the principle of material indifference [28, p. 288].

The problem is supplemented by the traction-free boundary conditions:

$$\mathbf{T}(\mathbf{x}) \cdot \mathbf{n}(\mathbf{x}) = \mathbf{0}, \quad \mathbf{x} \in \partial \mathcal{B}, \quad (2.5)$$

where \mathbf{n} is a unit vector field normal to the boundary. For a given strain-energy density function W and natural density ρ_0 , the solutions of Eqns (2.1–2.5) give the stresses and deformations at an equilibrium in which the gravitational forces are balanced by the internal forces due to elastic deformations. It was proved that this system has unique solutions for constant natural density and small strains [30] and for arbitrary deformations and constant natural density if the strain-energy density function satisfies some growth conditions [31].

(b) Spherical equilibria of a spherical elastic body

Next, we specialise the problem to the case of spherical deformations. We assume that in the absence of gravity the body is a homogeneous sphere of radius R_0 and constant density ρ_0 (Fig. 2). A material point is denoted by its spherical coordinates $\{R, \Theta, \Phi\} \in [0, R_0] \times [0, 2\pi] \times [0, \pi]$ in the reference configuration and by $\{r, \theta, \phi\} \in [0, r_0] \times [0, 2\pi] \times [0, \pi]$ in the current configuration. We choose a family of elastic materials of the form

$$W = \frac{\mu}{2}(I_1 - 3 - 2f_\alpha(J)) + \frac{\lambda}{2}(J - 1)^2. \quad (2.6)$$

Here $I_1 = \text{Tr}(\mathbf{C})$, is the principal invariant associated with the right Cauchy-Green tensor $\mathbf{C} = \mathbf{F}^T \mathbf{F}$, and μ, λ are non-zero constants. In small deformations, the parameters (μ, λ) can be identified with the Lamé parameters (μ, λ) . These parameters are related to Young's modulus E and Poisson's ratio ν through $\mu = E/(2(1 + \nu))$ and $\lambda = E\nu/((1 + \nu)(1 - 2\nu))$. The compressibility

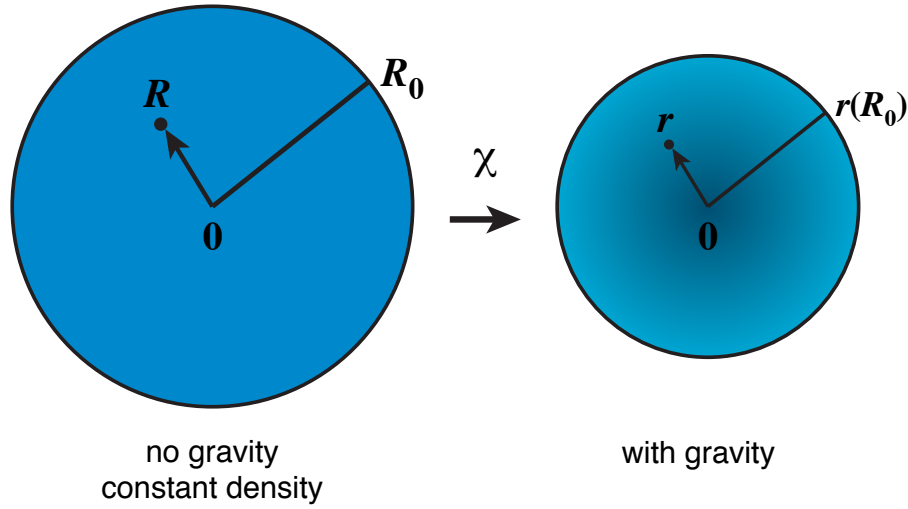


Figure 2. Spherical deformation of a spherical planet under its own gravity field.

penalty is

$$f_\alpha(J) = \ln J - \alpha \frac{(J-1)^4}{J^\alpha}. \quad (2.7)$$

We remark that this particular strain-energy density in the particular case $\alpha = 0$ is well known [32], but the general case for arbitrary α has been designed to offer a range of behaviours in large compression with the requirement that as α varies, the parameters (μ, λ) are independent of α .

Spherically symmetric deformations are of the form

$$r = r(R), \quad \theta = \Theta, \quad \phi = \Phi, \quad (2.8)$$

with a deformation gradient [28, p.273]

$$\mathbf{F} = \text{diag}(F_{rR}, F_{\theta\Theta}, F_{\phi\Phi}) = \begin{bmatrix} r'(R) & 0 & 0 \\ 0 & r/R & 0 \\ 0 & 0 & r/R \end{bmatrix}. \quad (2.9)$$

Once the strain-energy density function is defined, the Cauchy stress tensor is

$$\mathbf{T} = J^{-1} \mathbf{F} \frac{\partial W}{\partial \mathbf{F}} = \frac{\mu}{J} \mathbf{F} \mathbf{F}^\top + \frac{\partial W}{\partial J} \mathbf{1} \quad (2.10)$$

where

$$\frac{\partial W}{\partial J} = [-\mu f'_\alpha(J) + \lambda(J-1)]. \quad (2.11)$$

The Cauchy stress tensor written in the usual spherical coordinates takes the form $\mathbf{T} = \text{diag}(T_{rr}, T_{\theta\theta}, T_{\phi\phi})$ where

$$\begin{aligned} T_{rr} &= \frac{\mu}{J} F_{rR}^2 + \frac{\partial W}{\partial J}, \\ T_{\theta\theta} &= T_{\phi\phi} = \frac{\mu}{J} F_{\theta\Theta}^2 + \frac{\partial W}{\partial J}. \end{aligned} \quad (2.12)$$

Then, the only non-identically-vanishing equilibrium equation from (2.2) is

$$\frac{\partial T_{rr}}{\partial r} + \frac{2(T_{rr} - T_{\theta\theta})}{r} - \rho h_r = 0, \quad h_r = \frac{GM}{r^2}, \quad (2.13)$$

where M is the total mass within a sphere centred at origin with radius r . From mass conservation, we have

$$M = \frac{4}{3}\pi R^3 \rho_0, \quad \rho = J^{-1} \rho_0. \quad (2.14)$$

Therefore, we have

$$\frac{1}{r'(R)} \frac{\partial T_{rr}}{\partial R} + \frac{2(T_{rr} - T_{\theta\theta})}{r} - \frac{4}{3} \frac{J^{-1} G \pi R^3 \rho_0^2}{r^2} = 0. \quad (2.15)$$

There are two important dimensionless parameters that appear in the problem:

$$\xi = \frac{\lambda}{\mu}, \quad \eta = \frac{4\pi G R_0^2 \rho_0^2}{\mu} \quad (2.16)$$

The parameter ξ represents the relative elasticity of the material (as $\xi \rightarrow \infty$, the system becomes incompressible) and the parameter η represents the relative effect of gravity and elasticity. For most rocks, the Poisson ratio is between 0.2 and 0.3 and we use in our examples the value $\xi = 1$ corresponding to $\nu = 1/4$. Variations of the parameter ξ within known ranges does not change the qualitative behaviour of the solution. Larger values of η correspond to larger and/or denser planets for a given material or, equivalently, planets of similar sizes and density but made out of material with lower stiffness (η increases as the Young's modulus decreases). This parameter will be our main control parameter as we are interested in the change of equilibria for planets of increasing size. This parameter is also related to the ratio of two velocities: the escape velocity of a point on the surface is $v_{\text{esc}} = \sqrt{2gM/R_0}$ and the velocity of shear waves is given by $v_S = \sqrt{\mu/\rho_0}$. We have

$$\eta = \frac{3}{2} \frac{v_{\text{esc}}^2}{v_S^2}. \quad (2.17)$$

Without loss of generality we scale all lengths with the reference radius R_0 . Thus $r := r/R_0$ and $R := R/R_0$. Substituting (2.12) into (2.15), the equilibrium equation for $r = r(R)$ is

$$\begin{aligned} & \left[3R^5 r^2 - 3Rr^6 (f''_{\alpha}(J) - \xi) \right] r'' - 6Rr^5 (f''_{\alpha}(J) - \xi) r'^2 \\ & + \left[6R^4 r^2 + 6r^6 (f''_{\alpha}(J) - \xi) \right] r' - 6R^3 r^3 - \eta R^8 = 0. \end{aligned} \quad (2.18)$$

The boundary conditions are $r = R = 0$ at the center, and no traction at the surface $R = 1$, which gives $T_{rr}|_{R=1} = 0$ or

$$\left(-f'_{\alpha}(J) - \xi + \frac{(\xi r^4 + 1) r'}{r^2} \right) \Big|_{R=1} = 0. \quad (2.19)$$

Recalling that $J = r'(R)r^2/R^2$, we see that the equation for the equilibrium leads to a nonlinear second-order boundary-value problem for $r = r(R)$. This problem has a singularity at $R = 0$, where the coefficient in front of the highest derivative vanishes. Therefore, the study of this equation requires particular care.

Close to the origin $R = 0$, we can expand the solution in power series

$$r = \sum_{i=0}^{\infty} c_{2i+1} R^{2i+1} = c_1 R + c_3 R^3 + \dots, \quad (2.20)$$

where c_1 is undetermined, and from (2.18) all higher order coefficients are functions of c_1 and the parameters. The first two such coefficients are:

$$\begin{aligned} c_3 &= \frac{\eta}{30c_1^2 (c_1^4 \xi - c_1^4 f''_{\alpha}(c_1^3) + 1)}, \\ c_5 &= \frac{\eta^2 \left(-34c_1^4 \xi + 25c_1^7 f_{\alpha}^{(3)}(c_1^3) + 34c_1^4 f''_{\alpha}(c_1^3) - 10 \right)}{12600c_1^5 (c_1^4 \xi - c_1^4 f''_{\alpha}(c_1^3) + 1)^3}. \end{aligned} \quad (2.21)$$

The parameter $c_1 \in [0, 1]$ defines a one-parameter family of solutions and our problem is to determine c_1 for given values of the parameters from the boundary condition (2.19) at $R = 1$. The limit $c_1 \rightarrow 1$ corresponds to the trivial case $\eta = 0$ and $r = R$, whereas the limit case $c_1 \rightarrow 0$ corresponds to the case where the center of the planet is maximally compressed.

3. Small strain analysis

In the absence of gravity, the only solution is the trivial one: $r = R$. Therefore, for small values of η we expect the series solution to remain valid up to $R = 1$ and we can use the boundary value condition to find c_1 . For comparison with the linear theory, we look for a solution of the form $r = c_1 R + c_3 R^3$. Then, the boundary condition at $R = 1$ is

$$-f'_\alpha \left((c_1 + c_3)^2 (c_1 + 3c_3) \right) + \frac{(c_1 + 3c_3) \left(\xi (c_1 + c_3)^4 + 1 \right)}{(c_1 + c_3)^2} = \xi. \quad (3.1)$$

Substituting (2.21) into (3.1), results in a nonlinear equation for c_1 . For η small, c_1 is close to 1:

$$c_1 = 1 - \frac{\eta(5\xi + 6)}{30(\xi + 2)(3\xi + 2)} + \mathcal{O}(\eta^2) \quad (3.2)$$

and the solution is

$$r = R - \frac{\eta R}{30(\xi + 2)} \left(\frac{5\xi + 6}{3\xi + 2} - R^2 \right) + \mathcal{O}(\eta^2, R^5). \quad (3.3)$$

We can compare this solution with Love's solution [26, p.142] obtained from the theory of linear elasticity under the condition of constant density:

$$r_{\text{Love}} = R - \frac{g\rho R_0 R}{10\mu(\xi + 2)} \left(\frac{5\xi + 6}{3\xi + 2} - R^2 \right). \quad (3.4)$$

where $g\rho R_0/\mu = 4\pi G\rho^2 R_0^2(3/\mu) = \eta\rho^2/(3\rho_0^2) = \eta/(3J^2)$. Hence we have

$$\frac{g\rho R_0}{\mu} = \frac{\eta}{3} + \mathcal{O}(\eta^2, R^4), \quad (3.5)$$

and

$$r_{\text{Love}} = R - \frac{\eta R}{30(\xi + 2)} \left(\frac{5\xi + 6}{3\xi + 2} - R^2 \right) + \mathcal{O}(\eta^2, R^5). \quad (3.6)$$

We see that the small strain solution obtained from nonlinear elasticity theory recovers Love's solution. The problem is now to understand the behaviour of the solutions for larger values of η . Our strategy is to perform a complete analysis of the case $\alpha = 0$ and then consider the effect of compressibility by increasing the exponent α .

4. Large strain analysis

In this section, we discuss the solutions of (2.18) when $\alpha = 0$. In this case, (2.18)

$$\begin{aligned} 3Rr^2 \left[(R^4 + \xi r^4)r'^2 + R^4 \right] r'' + 6\xi Rr^5 r'^4 + 6(R^4 r^2 - \xi r^6)r'^3 \\ + (-\eta R^8 + 6R^5 r - 6R^3 r^3)r'^2 - 6R^4 r^2 r' = 0, \end{aligned} \quad (4.1)$$

with boundary conditions

$$r = 0 \quad \text{at } R = 0, \quad (4.2)$$

$$\left(\frac{1}{r^2} + \xi r^2 \right) r'^2 - \xi r' - \frac{1}{r^2} = 0, \quad \text{at } R = 1. \quad (4.3)$$

(a) Numerical method

We start our analysis by performing a numerical exploration of the solution for increasing values of η . We note that to the boundary-value problem (4.1-4.3) has a singularity at $R = 0$. Therefore, we use the truncated Taylor expansion $r = c_1 R + c_3 R^3$ close to the origin with

$$c_3 = \frac{\eta}{30(c_1^6 \xi + c_1^2 + 1)}. \quad (4.4)$$

For a fixed η and ξ , we choose $0 < \delta \ll 1$, then $r_\delta = r(\delta)$ and $r'_\delta = r'(\delta)$ are known from the expansion up to a single unknown c_1 . We can then use (r_δ, r'_δ) as an initial condition for a shooting problem where we integrate the solution up to $R = 1$ and solve the boundary condition (4.3) for c_1 . Once c_1 is known, the solution $r = r(R; \eta, \xi)$ is known numerically.

We use this shooting method for $\xi = 1$ and $\delta \ll 1$ and plot the possible values of $r(1)$ as a function of η as shown in Fig. 3. For η small, we see that the small strain solution (3.3) is accurate. However, for larger values of η the solutions are different and several interesting features can be observed.

First, there is a maximal value of $\eta = \eta_{\max} \approx 6.75$ after which no solution to the boundary-value problem can be found. Physically, this is the point at which *gravitational collapse* first occurs. The energy penalty due to compression is not sufficient to counteract the decrease of energy, the planet cannot support its own weight and collapse into a single point, a highly singular solution of the problem.

Second, we see that η_{\max} is also a branch point and for values of η close to but less than η_{\max} there are two possible solutions to the equilibrium equation. Mathematically, this is not unexpected as many nonlinear boundary-value problems are known to have multiple solutions.

Third, as we keep following the equilibrium branch, we see that a second branch point appears at $\eta \approx 3.09$. For values of η slightly larger than 3.09, three solutions exist as shown in Fig. 4. Following this branch, a third branch point appears, and so on. We observe that there are regions of parameters with 0, 1, 2, 3, 4, 5 equilibria and it is not a great leap of the imagination to suspect that this process will repeat itself indefinitely. Numerically the accumulation point of this spiral is found by taking the limit $c_1 \rightarrow 0$ at which we obtain $\eta_0 \approx 3.7723$. The accumulation point corresponds to an asymptotic behaviour where the local behaviour of the solution close to 0 changes from $r \sim R$ to $r \sim R^3$. We can use this observation and the fact that c_1 is small to obtain a full picture of the solution close to the accumulation point. We note that the limiting behaviour $r \sim R^3$ leads to a solution with $J \rightarrow 0$ at the origin. However, this solution still has finite strain energy in any neighborhood of the origin and is therefore a valid solution of the problem (see [33] and references therein for other singularities appearing in solid mechanics).

(b) Analytical solution around the accumulation point

Here, we analyse the solution when η is close to the accumulation point η_0 . In this case, c_1 is close to 0 and we define $c_1 = \epsilon \ll 1$. Using matched asymptotic expansion method, we first try to find the inner solution $r(R)$ around $R = 0$. This solution can be expressed as

$$r = \epsilon R + b_3 R^3 + b_5 R^5 / \epsilon + \mathcal{O}(\epsilon^{-2}), \quad (4.5)$$

where b_i are the parameters with leading order $\mathcal{O}(1)$. By introducing a boundary-layer coordinate

$$\tau = R / \epsilon^{\frac{1}{2}}, \quad (4.6)$$

we have $r(\tau) = \epsilon^{\frac{3}{2}} Y(\tau)$. Substituting (4.6) into (4.1), and solving for the leading order yields

$$3\tau Y^2 Y'' - \eta \tau^4 Y'^2 + 6\tau Y Y'^2 - 6Y^2 Y' = 0. \quad (4.7)$$

There is an exact solution to (4.7)

$$Y = \frac{\eta \tau^3}{6}, \quad (4.8)$$

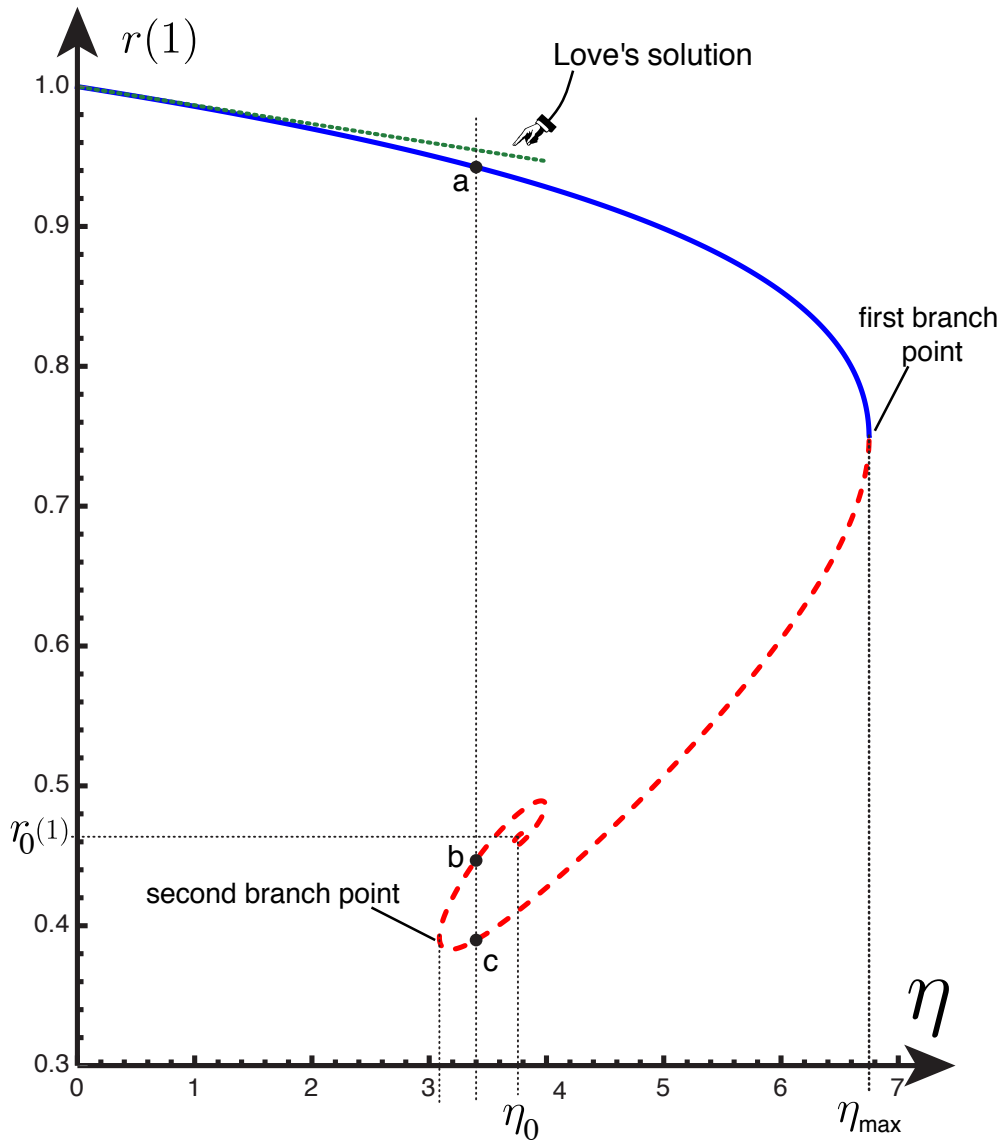


Figure 3. Current radius $r(1)$ as a function of increasing gravity η for $\xi = 1$ ($\delta = 10^{-4}$). The point at which gravitational collapse first appears is $\eta_{\max} \approx 6.75$ and the accumulation point is found at $\eta_0 \approx 3.77$. The dashed part of the curve represents solutions that are dynamically unstable. The three solution profile (a,b,c) $r(R)$ for $\eta = 3.4$ are shown in Fig. 4.

which does not satisfy the boundary condition at the origin. Locally near $\tau = 0$ the solution looks like

$$Y \sim \tau + \frac{\eta\tau^3}{30} + \mathcal{O}(\tau^5). \quad (4.9)$$

But every solution looks like $\eta\tau^3/6$ at infinity. The perturbation to the behaviour at infinity is given by

$$Y = \frac{\eta\tau^3}{6} + g(\tau), \quad (4.10)$$

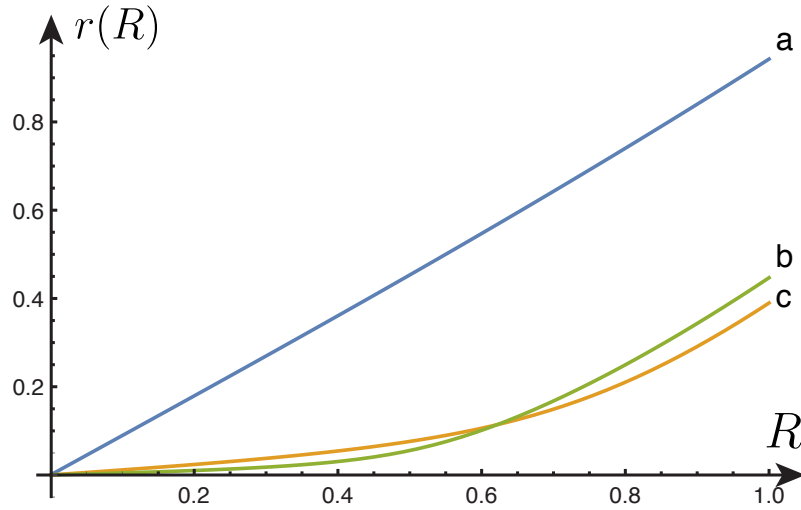


Figure 4. The three different solutions $r(R)$ for $\xi = 1$ and $\eta = 3.4$ associated with the three points a,b,c of Fig.1. The values of the parameter c_1 are 0.8944 (a), 0.0458 (b), 0.1145 (c). The solutions (b) and (c) are dynamically unstable

where, substituting (4.10) into (4.7) and linearising in $g(\tau)$,

$$\tau^2 g'' - 2\tau g' + 18g = 0. \quad (4.11)$$

Therefore,

$$g(\tau) = A\tau^{3/2} \cos\left(\frac{3}{2}\sqrt{7} \ln \tau + \gamma\right), \quad (4.12)$$

where A and γ are arbitrary constants. The inner solution with $Y(0) = 0$, $Y'(0) = 1$ will have this behaviour at infinity with some determined constants A and γ . We need to see what effect they have on the outer solution.

The perturbation to the outer solution is $o(\epsilon^{3/4})$ and we write

$$r = r_0 + \epsilon^{3/4} r_1 + o(\epsilon^{3/4}), \quad \eta = \eta_0 + \epsilon^{3/4} \eta_1 + o(\epsilon^{3/4}), \quad (4.13)$$

where r_0 is the special solution satisfying $r_0 \sim \eta R^3/6$ as $R \rightarrow 0$ and η_0 is the accumulation point (see Fig. 3). The equation for r_1 is

$$\alpha_1 r_1'' + \alpha_2 r_1' + \alpha_3 r_1 + \alpha_4 \eta_1 = 0, \quad (4.14)$$

where

$$\begin{aligned} \alpha_1 &= 3R^5 r_0'^2 r_0'' + 3R^5 r_0''^2 + 3\xi R r_0^6 r_0'^2, \\ \alpha_2 &= -18\xi r_0^6 r_0'^2 - 2\eta_0 R^8 r_0' + 6R^5 r_0^2 r_0' r_0'' + 12R^5 r_0 r_0' \\ &\quad + 18R^4 r_0^2 r_0'^2 - 6R^4 r_0''^2 - 12R^3 r_0^3 r_0' + 6\xi R r_0^6 r_0' r_0'' \\ &\quad + 24\xi R r_0^5 r_0'^3, \\ \alpha_3 &= -36\xi r_0^5 r_0'^3 + 6R^5 r_0 r_0'^2 r_0'' + 6R^5 r_0'^2 + 6R^5 r_0 r_0'' \\ &\quad + 12R^4 r_0 r_0'^3 - 12R^4 r_0 r_0' - 18R^3 r_0^2 r_0'^2 \\ &\quad + 18\xi R r_0^5 r_0'^2 r_0'' + 30\xi R r_0^4 r_0'^4, \\ \alpha_4 &= -R^8 r_0'^2 \end{aligned}$$

The inner (4.10) written in terms of the outer is

$$\begin{aligned} r &= \epsilon^{\frac{3}{2}} Y = \epsilon^{\frac{3}{2}} \left(\frac{\eta \tau^3}{6} + g \right) \\ &\sim \frac{\eta R^3}{6} + A \epsilon^{3/4} R^{3/2} \cos \left[\frac{3}{2} \sqrt{7} \ln \left(\frac{R}{\sqrt{\epsilon}} \right) + \gamma \right]. \end{aligned} \quad (4.15)$$

Thus

$$r_1 \sim \frac{\eta_1 R^3}{6} + A R^{3/2} \cos \left[\frac{3}{2} \sqrt{7} \ln \left(\frac{R}{\sqrt{\epsilon}} \right) + \gamma \right], \quad (4.16)$$

as $R \rightarrow 0$. At $R = 1$ we have

$$\alpha_5 r_1' + \alpha_6 r_1 = 0, \quad (4.17)$$

where

$$\begin{aligned} \alpha_5 &= -\xi + 2\xi r_0' r_0' + \frac{2r_0'}{r_0^2}, \\ \alpha_6 &= 2\xi r_0 r_0'^2 - \frac{2r_0'^2}{r_0^3} + \frac{2}{r_0^3}. \end{aligned}$$

We have to choose η_1 so that this condition is satisfied.

In summary, we can deduce $\eta_1(\epsilon)$ from (4.14), (4.16) and (4.17), where every constant is known and fixed. We can determine the dependence on ϵ as follows. Let $y(R)$ be a particular solution satisfying

$$\alpha_1 y'' + \alpha_2 y' + \alpha_3 y + \alpha_4 = 0, \quad (4.18)$$

with

$$\alpha_5 y' + \alpha_6 y = 0 \quad \text{at } R = 1 \quad (4.19)$$

and

$$y \sim B R^{3/2} \cos \left(\frac{3\sqrt{7}}{2} \ln R \right) \quad \text{as } R \rightarrow 0, \quad (4.20)$$

for some B . The inhomogeneity in the equation means we cannot set the amplitude, but we can impose the phase as $R \rightarrow 0$. Also let $z(R)$ be the homogeneous solution satisfying

$$\alpha_5 z' + \alpha_6 z = 0 \quad \text{at } R = 1, \quad (4.21)$$

and

$$z \sim A R^{3/2} \cos \left(\frac{3\sqrt{7}}{2} \ln R + \psi \right) \quad \text{as } R \rightarrow 0, \quad (4.22)$$

for some ψ , where A is as before. Here we are free to set the amplitude of z but not the phase. Then the solution r_1 is given by

$$r_1 = \eta_1 y + \zeta z, \quad (4.23)$$

where, in order to satisfy the matching conditions as $R \rightarrow 0$,

$$\begin{aligned} \eta_1 B + \zeta A \cos \psi &= A \cos \left(-\frac{3\sqrt{7}}{4} \ln \epsilon + \gamma \right), \\ -\zeta A \sin \psi &= -A \sin \left(-\frac{3\sqrt{7}}{4} \ln \epsilon + \gamma \right). \end{aligned} \quad (4.24)$$

Eliminating ζ from these last two relations gives

$$\begin{aligned} \eta_1 B &= \frac{A}{\sin \psi} \left[-\sin \left(-\frac{3\sqrt{7}}{4} \log \epsilon + \gamma \right) \cos(\psi) + \cos \left(-\frac{3\sqrt{7}}{4} \log \epsilon + \gamma \right) \sin(\psi) \right] \\ &= \frac{A}{\sin \psi} \sin \left(\psi - \gamma + \frac{3\sqrt{7}}{4} \log \epsilon \right). \end{aligned} \quad (4.25)$$

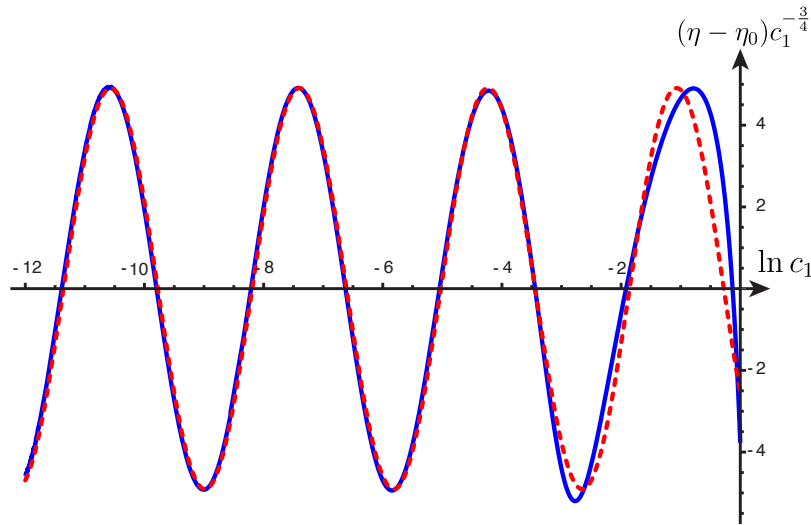


Figure 5. Asymptotic prediction (red/dashed) versus numerical results (blue/solid)

Thus

$$\eta = \eta_0 + c_1^{3/4} \frac{A}{B \sin \psi} \sin \left(\psi - \gamma + \frac{3\sqrt{7}}{4} \ln c_1 \right). \quad (4.26)$$

Numerically we find that $A = 0.473985$, $\gamma = 0.115302$, $\psi = 0.663228$, and $B = -0.156888$ for $\xi = 1$. The analytical results are compared with numerical results in Fig. 5. They match well when $c_1 < e^{-4}$. We conclude that there exist intervals for η where there are N equilibrium solutions for all integer N .

(c) Stability and vibrations

A natural question in the presence of multiple equilibria is to determine which ones are viable as physical solutions. To do so, we can test the stability of our spherical solutions against spherical vibrations. The equilibria for which these vibrations are imaginary are *unstable*. We refer to a planet as being *radially stable* if it is stable against radial disturbances (not precluding the possibility of the radial equilibrium being unstable against other, non-spherically symmetric, deformations). The radial dynamics of an elastic planet is governed by the Cauchy equation

$$\frac{\partial T_{rr}}{\partial r} + \frac{2(T_{rr} - T_{\theta\theta})}{r} - \rho h_r = \rho \ddot{r}, \quad (4.27)$$

The boundary conditions are, as before $r(0) = 0$ and $T_{rr} = 0$ at $R = 1$. We study the vibration around an equilibrium solutions, so that r has the form

$$r = r^{(0)}(R) + \epsilon \left(\varphi(R) e^{i\omega t} + c.c. \right). \quad (4.28)$$

where *c.c.* stands for the complex conjugate, $r^{(0)}(R)$ is an equilibrium solution and $\epsilon \ll 1$. We choose $r := r/R_0$, $R := R/R_0$, $\xi = \lambda/\mu$, and $\eta = 4G\pi R_0^2 \rho_0^2 / \mu$ as before, and rescale time so that $\omega := \omega R_0 \sqrt{\rho_0/\mu}$. Substituting (4.28) into (4.27) and keeping the leading order term in ϵ yields

$$\beta_1 \varphi'' + \beta_2 \varphi' + \beta_3 \varphi = 0 \quad (4.29)$$

with

$$\begin{aligned} \varphi = 0 \text{ at } R = 0, \text{ and} \\ \beta_4 \varphi' + \beta_5 \varphi = 0, \text{ at } R = 1. \end{aligned} \quad (4.30)$$

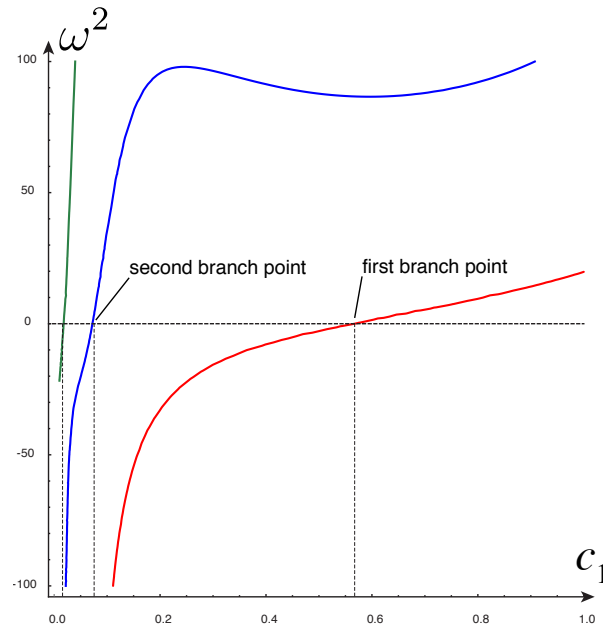


Figure 6. First three eigenvalues ω^2 as a function of c_1 .

where the coefficients, given explicitly in Appendix A, depend on the solution $r^{(0)}$ and the frequency ω through ω^2 . For a given equilibrium solutions, these equations are therefore an eigenvalue problem for ω^2 that can be solved by using the shooting method. We define

$$K(c_1, \omega^2) = \beta_4 \varphi'(1) + \beta_5 \varphi(1). \quad (4.31)$$

Since the equilibrium solutions can be parameterised by c_1 , a given c_1 defines a solution $r^{(0)}$ and we compute its spectrum by solving $K(c_1, \omega^2) = 0$ for ω^2 as shown in Fig. 6. We see that as c_1 decreases from 1, it reaches $c_1 \approx 0.568$ where the smallest eigenvalue ω^2 becomes negative. This value corresponds to the first branch point found in Fig. 3. For $0 \leq c_1 \lesssim 0.568$, all equilibrium solutions are unstable. Similarly the value of c_1 where the second smallest eigenvalue becomes negative corresponds to the second branch point shown in Fig. 3.

5. The role of compressibility

Next, we turn our attention to the case $\alpha > 0$ to gauge the role of the energy penalty associated with changes in volume. In particular we are interested to see if there is a critical value at which gravitational collapse is not possible and a unique solution exists for all η . Equivalently, we can compute the value of α at which the first branch point disappears. We use the AUTO continuation software [34] to solve (2.18–2.19). For a given value of α we compute

$$r_\infty(\alpha) = \lim_{c_1 \rightarrow 0} r(1). \quad (5.1)$$

The result of this computation is shown in Fig. 7. For small values of α we observe the same qualitative behaviour as described in the previous sections. Around $\alpha_1 \approx 0.20$, there is a qualitative change of behaviour and a positive r_∞ is replaced by r_∞ close to 0. For $\alpha \in [\alpha_2, \alpha_3]$ with $\alpha_2 \approx 0.34$ and $\alpha_3 \approx 0.54$, there are 1, 2, or 3 solutions as shown in Fig. 8. This behaviour changes again when the branch point disappears and there is a unique solution for all values of η . Interestingly, in this regime, the final radius of the planet becomes independent of the size of the planet as the final radius becomes independent of the total mass for sufficiently large planets.

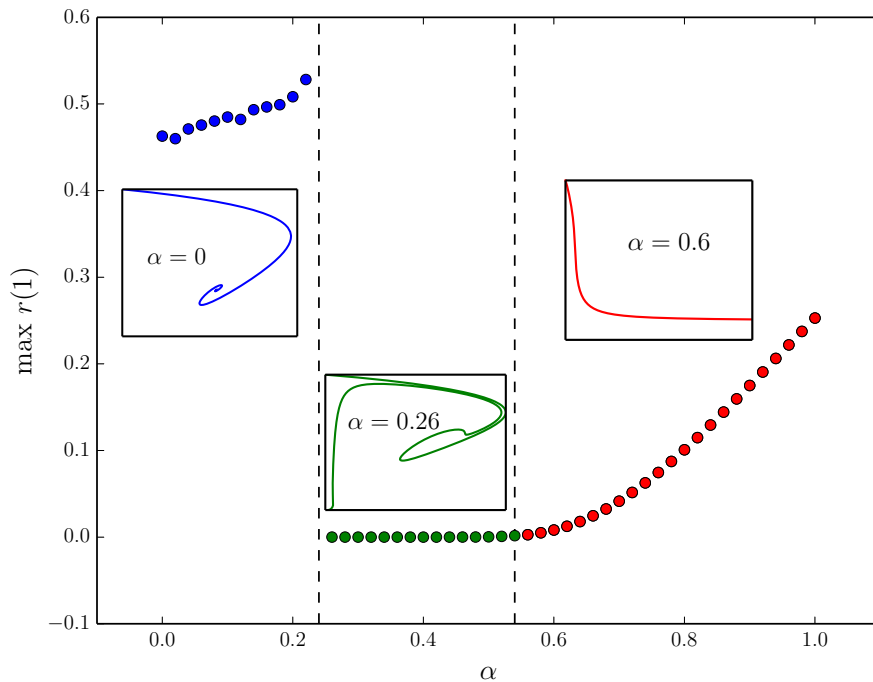


Figure 7. Effect of α on the existence of equilibria: $r_\infty(\alpha)$ is shown as a function of α . For $\alpha \in [0, 0.22]$ the bifurcation diagram is spiral as in the $\alpha = 0$ case. For $\alpha \in [0.22, 0.54]$, this spiral unwinds. For $\alpha \in [0.54, 1]$, a single solution exists for all values of η .

(a) Stability results for general α

From Eqs.(4.29) and (4.30), we can probe the stability of equilibria for general α by finding the loci at which the eigenvalues ω^2 vanish as a function of c_1 and α . This analysis confirms that the upper branch of solutions (as shown in Fig. 3 and Fig. 8) is always radially stable up to the first branch point at which the equilibrium solution becomes unstable. Similarly, when there exists a solution for large values of η (as in Fig. 8), this lower branch is also radially stable up to the first branch point. Therefore, for $\alpha > 0.54$ all solutions are radially stable. The intermediate case $\alpha \in [0.34, 0.54]$ leads to two radially stable branches with an overlap, offering the possibility of bistability, another unexpected feature of this celestial problem.

6. Conclusion

The problem of determining the deformation of a continuum body under its own gravitational field is a classic problem of continuum mechanics. Despite a wealth of knowledge for the fluid case, surprisingly little is known about the solid case for which even the simplest question of finding the radius of a deformed homogeneous elastic planet has not been thoroughly investigated. Here, as a starting point, we considered a particular elastic model and posed the problem in large deformations without any approximation. We further specialised our analysis to the existence of radially symmetric solution leading to a second-order boundary-value problem for the radial deformation. The study of this equation was performed by combining asymptotic methods with numerical methods to obtain a global picture of how solutions behave for planets of increasing size. Our study identified a number of surprising features.

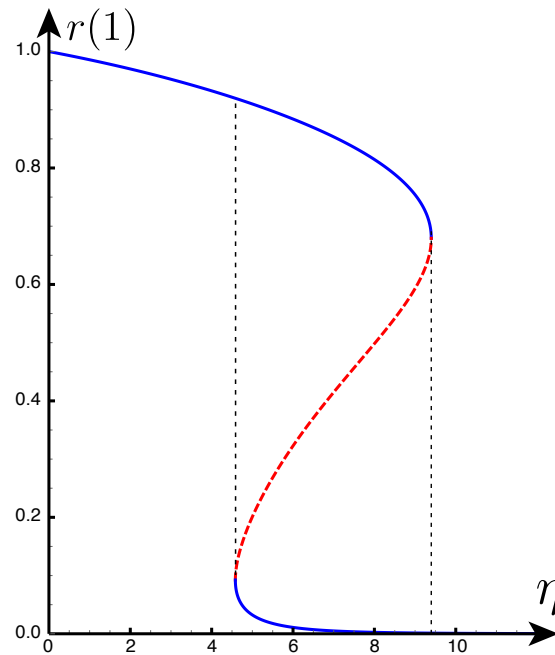


Figure 8. For $\alpha = 0.4$, the system can have up to three solutions, two of which are radially stable, showing the possibility of bistability.

First, we observed the possibility of gravitational collapse. At a critical size, the gravitational field cannot be balanced by internal elastic forces and the planet collapses to a point despite the fact that the elastic energy diverges in that limit. We note that Love already discussed this possibility within the framework of linear elasticity (where the elastic energy remains finite as the volume vanishes) [23]. Clearly, gravitational collapse of this type would not be expected for an actual planet where levels of high compression would require other physical effects (such as phase transitions) and for which an elastic model would not be suitable. Even, within the elastic context, we found that if the elastic potential diverges sufficiently fast as the volume vanishes (as measured by our parameter α), gravitational collapse disappears and is replaced by a monotonic behaviour with a single solution for all planet sizes.

Second, we found that in some elastic models, there may be arbitrarily many elastic equilibria. Each of these is a valid solution of the exact equations. In these cases, by following the branch of solutions we reach an accumulation point η_0 for which infinitely many solutions can co-exist, as confirmed by a local asymptotic expansion in the neighbourhood of η_0 . This phenomenon is again dependent on the singular behaviour of the solutions as the volume vanishes at the origin. Indeed, it corresponds to the limiting behaviour $r \sim c_1 R$ at the origin in the limit $c_1 \rightarrow 0$ so that $r \sim R^3$ and $J \rightarrow 0$ at the origin. This transition can be controlled by increasing the exponent α and for $\alpha > 0.54$ only a single radial solution exists.

Third, we studied the stability of our multiple equilibria. Not surprisingly, we found that instability is naturally associated with the existence of branch points in the bifurcation diagram. At each branch point a new eigenvalue of the radial dynamical linearised problem becomes imaginary leading to dynamically unstable solutions. Further analyses showed that small elastic planets (small η) are always radially stable, and so are very large planets (large η), when they exist. The existence of two stable branch leads to the possibility of bistability when there is an overlap of these branches as shown in Fig. 8.

How realistic is an elastic model for a planet? For small enough deformations, every solid behaves elastically and there is no doubt that an elastic model is relevant and linear elasticity

can be used. When does linear elasticity fail to properly determine the stresses? This is a difficult question that can only be addressed by comparing the linear theory to a nonlinear theory as presented here. In any case, for larger deformations, the elastic assumption will fail as other effects, such as phase transition, may come into play. Yet, stresses are needed to determine these transitions. Hence the elastic model is required. Simple estimates for planets are very difficult since very little is known about their composition and structure. For instance, it is not clear that the theory presented here would be valid for the Earth that is known to have a complex core. Yet, we can try to apply our theory to the problem of iron planets such as Mercury. In this case we have $\mu \approx 80\text{GPa}$, $\rho_0 \approx 7860\text{kg/m}^3$, so that $\xi \approx 1.5$ and $\eta = 4G\pi R_0^2 \rho_0^2 / \mu \approx (8.04 \times 10^{-7} R_0)^2 = (k_0 R_0)^2$. For $\alpha = 0$, we obtain an estimate of $\eta_{\max} \approx 7.77$ corresponding to a maximal radius of $2.25/k_0 \approx 2,798\text{ km}$ (compared to the actual radius of Mercury at 2,440km). We should not read too much in the closeness of these values since many other effects may be involved and we do not expect that gravitational collapse as presented here would be directly applicable to actual planets. Nevertheless, this estimate suggests that some planets may be subject to large elastic deformations and that speculations on the composition of planets based on linear theories, as prevalent in all geosciences, should be reconsidered critically.

The stability notion used here only concerns radial disturbances. It does not preclude the possibility that a planet could become unstable by developing non-radially symmetric modes at a given size. This type of behaviour was found by Love in 1907 but then ruled out later by Jeans in 1915. In both instances, the assumptions made were unphysical and the problem was studied within the linear setting. From a modern perspective, the simple question of stability of planets under their own gravitational field remains open and will be the subject of the second instalment of this work.

In our study, we have removed, on purpose, many secondary effects that may be important for the modelling of actual planets. For instance, we have neglected the gravitational interaction with other bodies, the forces associated with rotation, the possibility that the planet core may be a viscous fluid, the role of thermal stresses, the distribution of continents, and all non-elastic effects such as plastic yielding, rupture, and so on. These effects may all be critical in determining the figure of a given planet but we claim that their relative roles can only be appreciated once the simpler problem considered here is fully understood. In turn, a general theory should offer new insight into the surprising gravitational behaviour of heavenly bodies.

Data accessibility statement: This work does not have any experimental data.

Competing interests statement. We have no competing interests.

Funding: This work is supported by the National Natural Science Foundation of China (Grants No. 11772276 and No. 11402217), and the Chinese Consulate General (Grant No. 201709390003). The support for Alain Goriely by the Engineering and Physical Sciences Research Council of Great Britain under research grant EP/R020205/1 is gratefully acknowledged.

Author's contribution: AG conceived the model and formulated the problem. AG, SC, FJ, and KO studied the solutions numerically and analytically. All authors contributed to the writing of the document. All authors gave final approval to the document.

Acknowledgments: The original formulation of the problem considered here results from discussions and collaborations between AG and Michael Tabor at the University of Arizona and his critical help in shaping this problem is gratefully acknowledged.

A. Coefficients of the linearised vibration problem

The vibration problem is given by

$$\beta_1 \varphi'' + \beta_2 \varphi' + \beta_3 \varphi = 0 \quad (\text{A } 1)$$

with

$$\begin{aligned} \varphi = 0 \text{ at } R = 0, \text{ and} \\ \beta_4 \varphi' + \beta_5 \varphi = 0, \text{ at } R = 1. \end{aligned} \quad (\text{A } 2)$$

where the coefficients

$$\begin{aligned} \beta_1 &= 3R^3 r^{(0)3} r^{(0)'} \left(r^{(0)4} (\xi - f''_\alpha(J_0)) + R^4 \right), \\ \beta_2 &= -6Rr^{(0)8} r^{(0)'}{}^3 f'''_\alpha(J_0) + 3r^{(0)9} r^{(0)'} f'''_\alpha(J_0) \left(2r^{(0)'} - Rr^{(0)''} \right) \\ &\quad + 6R^3 r^{(0)6} r^{(0)'}{}^2 (\xi - f''_\alpha(J_0)) + 3R^3 r^{(0)7} r^{(0)''} (f''_\alpha(J_0) - \xi) \\ &\quad + \eta R^{10} r^{(0)} - 3R^7 r^{(0)3} r^{(0)''} + 6R^5 r^{(0)4}, \\ \beta_3 &= r^{(0)'} \left[-12Rr^{(0)7} r^{(0)'}{}^3 f'''_\alpha(J_0) + 6r^{(0)8} r^{(0)'} f'''_\alpha(J_0) \left(2r^{(0)'} - Rr^{(0)''} \right) \right. \\ &\quad + 6R^2 r^{(0)6} \left(Rr^{(0)''} - 2r^{(0)'} \right) (\xi - f''_\alpha(J_0)) + 6R^3 r^{(0)5} r^{(0)'}{}^2 (\xi - f''_\alpha(J_0)) \\ &\quad \left. + 4\eta R^{10} - 6R^6 r^{(0)2} \left(Rr^{(0)''} + 2r^{(0)'} \right) + 3R^5 r^{(0)3} \left(R^2 \omega^2 + 2 \right) \right], \\ \beta_4 &= -r^{(0)5} f''_\alpha(J_0) + \xi r^{(0)5} + r^{(0)}, \\ \beta_5 &= 2r^{(0)'} \left(-r^{(0)4} f''_\alpha(J_0) + \xi r^{(0)4} - 1 \right), \\ J_0 &= J(r^{(0)}) \end{aligned}$$

In the particular case $\alpha = 0$, it reduces to

$$\begin{aligned} \beta_1 &= 3r^{(0)'} Rr^{(0)3} \left((1 + r^{(0)'}{}^2) R^4 + r^{(0)'}{}^2 r^{(0)4} \xi \right), \\ \beta_2 &= Rr^{(0)} \left(12r^{(0)'} R^3 r^{(0)2} - 9r^{(0)''} R^4 r^{(0)2} + 6r^{(0)'}{}^4 r^{(0)5} \xi + r^{(0)'}{}^2 (6R^2 r^{(0)3} \right. \\ &\quad \left. - 3R^4 r^{(0)} (2 + r^{(0)''} r^{(0)}) + R^7 \eta - 3r^{(0)''} r^{(0)6} \xi \right), \\ \beta_3 &= r^{(0)'} \left(12r^{(0)'} R^4 r^{(0)2} - 6r^{(0)''} R^5 r^{(0)2} + 6r^{(0)'}{}^4 Rr^{(0)5} \xi - 12r^{(0)'}{}^3 r^{(0)2} (R^4 + r^{(0)4} \xi) \right. \\ &\quad \left. + r^{(0)'}{}^2 (6R^3 r^{(0)3} + 4R^8 \eta \right. \\ &\quad \left. + 6r^{(0)''} Rr^{(0)6} \xi + 3R^5 r^{(0)} (-6 - 2r^{(0)''} r^{(0)} + r^{(0)2} \omega^2) \right) \end{aligned}$$

With boundary condition at $R = 1$

$$r^{(0)} \left(r^{(0)'}{}^2 (\xi r^{(0)4} + 1) + 1 \right) \varphi' + 2 \left(r^{(0)'}{}^3 (\xi r^{(0)4} - 1) + r^{(0)'} \right) \varphi = 0, \quad (\text{A } 3)$$

while at $R = 0$, $\varphi = 0$.

References

1. Birch F. 1939 The variation of seismic velocities within a simplified earth model, in accordance with the theory of finite strain. *Bulletin of the Seismological Society of America* **29**, 463–479.
2. Sawyers KN, Rivlin RS. 1969 Seismic Wave Propagation in a Self-Gravitating Anisotropic Earth. *Philosophical Transactions of the Royal Society of London Series a-Mathematical and Physical Sciences* **263**, 615–&.
3. Walton K. 1974 The Seismological Effects of Elastic Pre-Straining within the Earth. *Geophysical Journal of the Royal Astronomical Society* **36**, 651–671.
4. Darwin GH. 1879 On the Bodily Tides of Viscous and Semi-Elastic Spheroids, and on the Ocean Tides upon a Yielding Nucleus. *Philosophical Transactions of the Royal Society of London* **170**, 1–35.
5. Holsapple KA, Michel P. 2006 Tidal disruptions: A continuum theory for solid bodies. *Icarus* **183**, 331–348.
6. Matsuyama I, Mitrovica JX, Manga M, Perron JT, Richards MA. 2006 Rotational stability of dynamic planets with elastic lithospheres. *Journal of Geophysical Research E: Planets* **111**, 1–17.
7. Matsuyama I, Nimmo F. 2007 Rotational stability of tidally deformed planetary bodies. *Journal of Geophysical Research E: Planets* **112**, 1–11.
8. Daradich A, Mitrovica JX, Matsuyama I, Perron JT, Manga M, Richards MA. 2008 Equilibrium rotational stability and figure of Mars. *Icarus* **194**, 463–475.
9. Farinella P, Milani A, Nobili AM, Paolicchi P, Zappala' V. 1983 The shape of the small satellites of Saturn: Gravitational equilibrium vs solid-state strength. *The Moon and the Planets* **28**, 251–258.
10. Wettlelauder JS. 2010 Accretion in protoplanetary disks by collisional fusion. *The Astrophysical Journal* **719**, 540.
11. de Maupertuis PLM. 1739 *La figure de la Terre déterminée*.
12. Todhunter I. 1873 *A History of the Mathematical Theories of Attraction and the Figure of the Earth: 1 vol. 1*. Macmillan.
13. Lebovitz NR. 1998 The mathematical development of the classical ellipsoids. *International Journal of Engineering Science* **36**, 1407–1420.
14. Holsapple KA. 2004 Equilibrium figures of spinning bodies with self-gravity. *Icarus* **172**, 272–303.
15. Chandrasekhar S. 1965 The Stability of a Rotating Liquid Drop. *Proceedings of the Royal Society A: Mathematical, Physical and Engineering Sciences* **286**, 1–26.
16. Chandrasekhar S. 1969 *Ellipsoidal figures of equilibrium*. Yale Univ. Press.
17. Williams IP. 2003 The Roche limit. *Celestial Mechanics and Dynamical Astronomy* **87**, 13–25.
18. Lacaze L, Le Gal P, Le Dizès S. 2004 Elliptical instability in a rotating spheroid. *Journal of Fluid Mechanics* **505**, 1–22.
19. Newton I. 1687 *Philosophiae naturalis principia mathematica*. London.
20. Jeans JH. 1903 On the Vibrations and Stability of a Gravitating Planet. *Proceedings of the Royal Society of London, Series A* **201**, 157–184.
21. Jeans JH. 1902 The Stability of a Spherical Nebula. *Philosophical Transactions of the Royal Society A: 199*, 1–53.
22. Jeans JH. 1917 Gravitational Instability and the Figure of the Earth. *Proceedings of the Royal Society of London. Series A* **93**, 413–417.
23. Love AEH. 1907 The Gravitational Stability of the Earth. *Proceedings of the Royal Society A: Mathematical, Physical and Engineering Sciences* **79**, 171–241.
24. Ekman M. 1993 A concise history of the theories of tides, precession-nutation and polar motion (from antiquity to 1950). *Surveys in Geophysics* **14**, 585–617.
25. Love AEH. 1963 *Some Problems of Geodynamics Being an Essay To Which the Adams Prize In the University of Cambridge Was Adjusted In 1911*. Cambridge University Press.
26. Love AEH. 1892 *A treatise on the mathematical theory of elasticity*. Cambridge University Press, Cambridge.
27. Landau LD, Lifshitz EM. 1959 *Theory of Elasticity*. Pergamon Press, Oxford.
28. Goriely A. 2017 *The Mathematics and Mechanics of Biological Growth*. Springer Verlag, New York.
29. Steinmann P. 2011 Geometrically nonlinear gravito-elasticity: Hyperelastostatics coupled to Newtonian gravitation. *International Journal of Engineering Science* **49**, 1452–1460.
30. Beig R, Schmidt BG. 2002 Static, Self-Gravitating Elastic Bodies. *Proceedings of the Royal Society of London A: Mathematical, Physical and Engineering Sciences* **459**, 109–115.

31. Calogero S, Leonori T. 2015 Ground states of self-gravitating elastic bodies. *Calculus of Variations and Partial Differential Equations* **54**, 881–899.
32. Ogden RW. 1984 *Non-linear Elastic Deformations*. Dover, New York.
33. Yavari A, Goriely A. 2015 On the stress singularities generated by anisotropic eigenstrains and the hydrostatic stress due to annular inhomogeneities. *J. Mech. Phys. Solids* **76**, 325–337.
34. Doedel EJ, Champneys AR, Fairgrieve TF, Kuznetsov YA, Sandstede B, Wang X et al.. 1998 Auto97. *Continuation and bifurcation software for ordinary differential equations*.